# Fiber Optic Distributed Sensing

**Alfredo Güemes, Antonio Fernandez-Lopez, Angel Lozano**
Dpt. Aeronautics, Univ. Politécnica de Madrid
Plaza Cardenal Cisneros, 3 MADRID 28040
SPAIN

Alfredo.guemes@upm.es, Antonio.fernandez.lopez@upm.es, angel.lozano@upm.es

## *ABSTRACT*

*Only recently available, the fiber optic distributed sensing technique is becoming a powerful tool for structural tests. Among the different techniques available, we were using OBR. The OBR uses swept wavelength interferometry (SWI) to measure the Rayleigh backscatter as a function of length in optical fiber with high spatial resolution. The SWI approach enables robust and practical distributed temperature and strain measurements in standard fiber with millimeter scale spatial resolution over hundreds of meters of fiber with strain and temperature resolution as fine as 1 microstrain and 0.1 °C. Structural damage detection from direct strain measurements can be done only when the sensors are very closely located to the damage initiation point, which is generally impossible to predict. With the availability of high resolution distributed sensing, strains along a continuous line can be obtained, so a crack crossing or growing near to the sensing line will be detected.*

## INTRODUCTION

FBG (Fiber Bragg Grating) sensors, have been used for the last 20 years, and they have built up a confidence in its performances. FBGs can measure the strain with a similar accuracy to the standard strain gages and extensometers, and they are also comparable in many aspects from a user's point of view. Indeed, their measurements are local and directional, they require compensation for temperature, they are commonly used by bonding them onto the surface, and even it is also possible to embed the optical fiber in the laminate in the case of composite structures. The main advantages of the FBG over the electrical strain gage are its reliability for long term measurements; because it is frequency coded, without drifting by aging, and its ability for multiplexing; since several FBGs can be engraved on the same fiber at different positions, resulting in the simultaneous measurement points. The most common procedure for multiplexing is to use a different central frequency for each grating, allowing up to ten FBGs in a single optical fiber, for conventional applications. Another multiplexing procedure is to have all the gratings with the same central frequency, with a low reflectivity; if gratings are adequately spaced, the return signal will be time-multiplexed, allowing a much larger number of sensors per fiber. The drawback of this procedure is that its response time is smaller, restricting the system to quasi-static applications.

Getting the strains all along the optical fiber length, with adequate spatial resolution and strain accuracy, opens new possibilities for structural tests and for structural health monitoring. This is what is understood as 'distributed sensing', with the main difference that the fiber does not need to have local engraved sensors.

The starting point of fiber optic distributed sensing may be identified at the beginning of the 1980s, with the Optical Time-Domain Reflectometer (OTDR) technology, a technique widely used for testing optical cables in the telecommunications industry. The concept is to send a narrow pulse of light through the optical fiber and keep listening for the 'echo' of the backscattered radiation. The detected signal provides a detailed picture of the local loss distribution or reflections along the fiber caused by any of the attenuation mechanisms or some other non-homogeneities on the fiber. The location of the defect may be calculated by the time of flight. The spatial resolution is in the range of meters, but the operating range was several kms,

so the technique has been found to be very useful for locating fiber breaks. Figure 1 illustrates the typical graph obtained with conventional equipments. Note the X scale is distance, in Km.

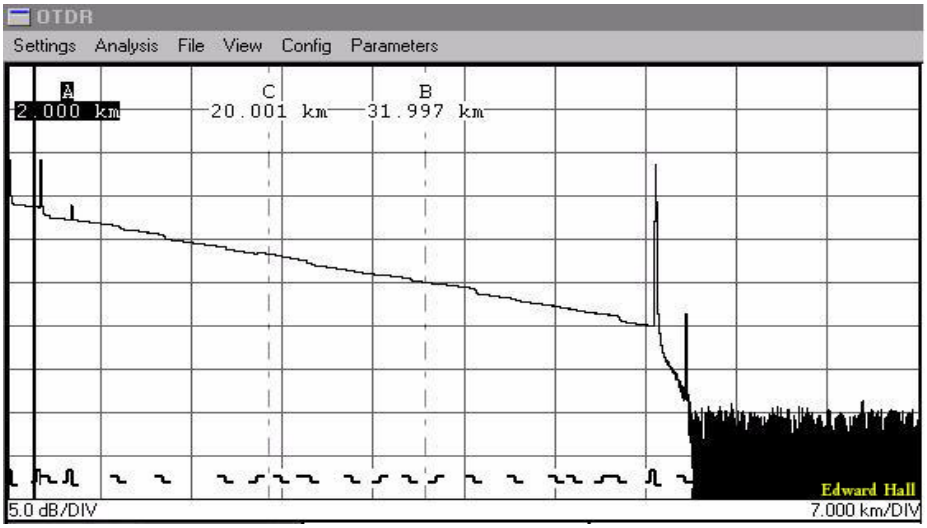


**Figure 1: Typical graph obtained with an OTDR, distance .VS. optical losses.**

## 1.0 THE BACKSCATTERED RADIATION

The backscattered light consists of different spectral components due to different interaction mechanisms between the propagating light pulse and the material of the optical fiber. These backscattered spectral components include Rayleigh, Brillouin, and Raman peaks or bands. The Rayleigh backscattering component is the strongest one, and it is due to density and composition fluctuations and has the same wavelength as the primary laser pulse. The Rayleigh component controls the main slope of the decaying intensity curve and may be used to identify the breaks and heterogeneities along the fiber.

A small percentage of photons interexchange energy with the atoms and new photons with lower (Stokes components) or higher energy are produced. This is known as Raman scattering, the spectral shift is related to the quantum energy absorption/desorption by the atomic bonds of the silica. The intensity of the anti-Stokes component of the Raman radiation increases with temperature, whilst the Stokes component remains stable; the power ratio between these two peaks, together with the time of arrival provides information about the local temperature and position respectively. Many commercial systems are currently available to obtain temperature maps over long distances, with important hydrological and environmental applications, including the detection of leakages in buried pipes. These systems basically use a pulsed laser for sending a high power short pulse along the fiber (spatial resolution is related to the width of the pulse, and can hardly be better than 1 meter); at the returning path there is a wavelength separation module, filtering every radiation distinct from the two Raman peaks, and fast photodetectors for each peak. Computing the time for the distance to the light source, and the relative height, resolution in temperature in the range of 0,1 ºC, for distances up to 50 km can be achieved.

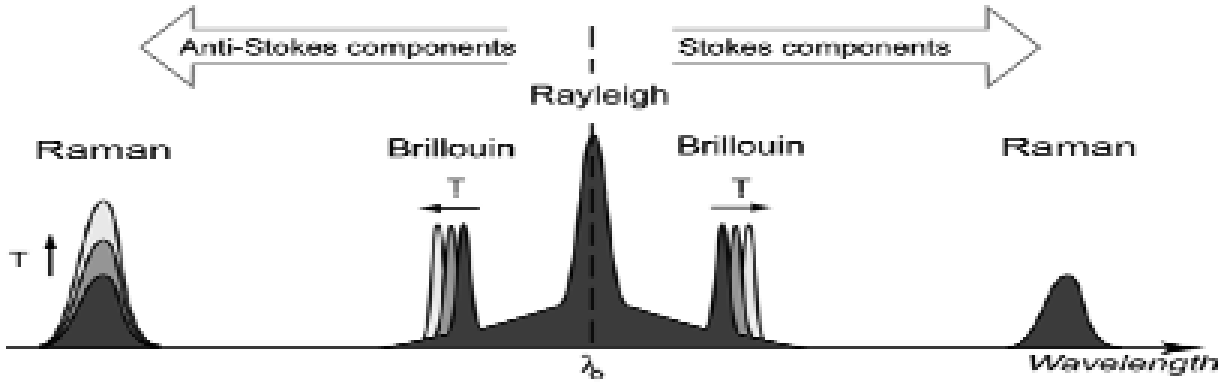


**Figure 2: Wavelengths of the backscattered radiation.**

Raman peaks height was insensitive to strain; in the case of the Brillouin scatter, the wavelength drifting is related to the local temperature and the strain in the fiber. Brillouin-based sensing techniques rely on the measurement of a frequency as opposed to Raman-based techniques which are intensity based. Brillouin based techniques are consequently inherently more accurate and more stable on the long term, since intensity-based techniques suffer from a higher sensitivity to drifts.

There are two types of Brillouin fiber optic sensors. Brillouin Optical Time Domain Reflectometers (BOTDR) resolves the strain or temperature based on Brillouin scattering of a single pulse. Brillouin Optical Time Domain Analysis (BOTDA) uses a more complicated phenomenon known as Stimulated Brillouin Scatter (SBS).

Brillouin scattering occurs as a result of an interaction between the propagating optical pulse and the acoustic waves present in the silica fiber, generating frequency shifted components. The diffracted light experiences a Doppler shift since the atoms vibrate at the acoustic velocity in the fiber. The acoustic velocity is directly related to the medium density and depends on both temperature and strain. The classical BOTDR is essentially an OTDR with a strong filter to avoid the Rayleigh radiation, and with an additional device to discriminate the wavelength of the Brillouin peak. Consequently, it will have the same advantages and limitations of OTDRs: very long interrogation distances, low spatial resolution.

Brillouin Optical Time Domain Analysis (BOTDA) uses a more complicated phenomenon known as Stimulated Brillouin Scatter (SBS). The typical sensor configuration requires two lasers that are directed in opposite directions through the same loop of fiber (one laser operating continuously, the other pulsed). When the frequency difference between the two lasers is equal to the "Brillouin frequency" of the fiber, there is a strong interaction between the 2 laser beams inside the optical fibers and the enhanced acoustic waves (phonons) generated in the fiber.

This interaction causes a strong amplification of the Brillouin signal which can be easily detected and localized using an OTDR-type sampling apparatus. To make a strain or temperature measurement along the fiber, it is necessary to map out the Brillouin spectrum by scanning the frequency difference (or "beat" frequency) of the two laser sources and fitting the peak of the Brillouin spectrum to get the temperature and strain information. Current existing BOTDA systems have a spatial resolution in the range of 10 cm, expecting to reach 1 cm in the next equipments generation.

## 2.0 THE OBR (OPTICAL BACKSCATTER REFLECTOMETRY)

The OBR uses swept wavelength interferometry (SWI) to measure the Rayleigh backscatter as a function of length in the optical fiber with high spatial resolution. An external stimulus (like a strain or temperature

change) causes temporal and spectral shifts in the local Rayleigh backscatter pattern. These temporal and spectral shifts can be measured and scaled to give a distributed temperature or strain measurement. The SWI approach enables robust and practical distributed temperature and strain measurements in standard fiber with millimeter-scale spatial resolution over tens to hundreds of meters of fiber with strain and temperature resolution as fine as 1 microstrain and 0.1 °C.

Figure 3 shows the high spatial resolution achieved. Imagine we have a fiber under test, with four partial reflectors. Each reflector forms an interferometer with the light that goes directly through the other arm of the first coupler. When the system is interrogated by a continuous tunable laser, the reflected signal from each partial reflector is modulated by a unique frequency, longer distances implies faster beatings. A Bragg grating sensor is a partial reflector, with a spectral width much wider that the beating of interferometry, as depicted. Using the Fourier transform, the position of each grating is obtained. With SWI, hundreds of FBG could be multiplexed in a single optical fiber.

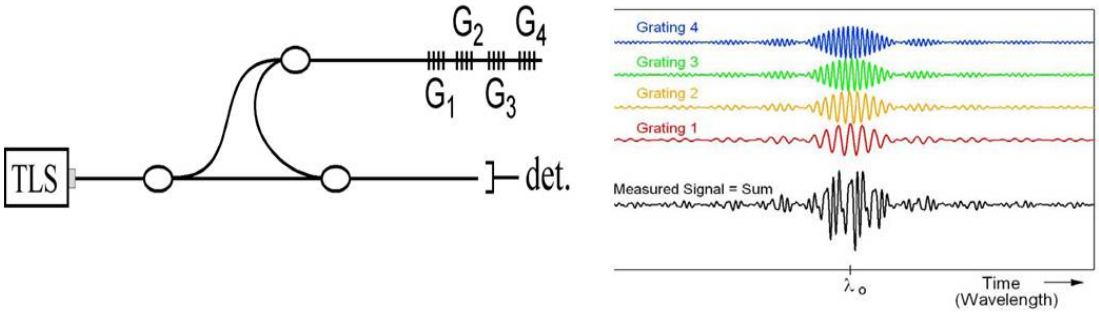


**Figure 3: Sketch of the SWI, and the obtained signals.**

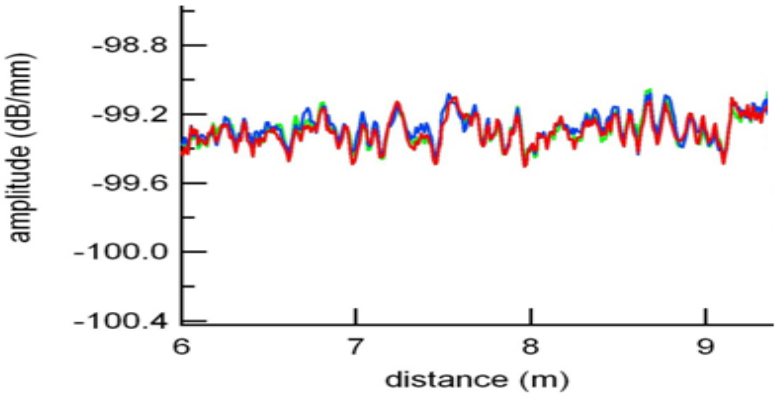


**Figure 4: Backscatter Light profile represents a fingerprint that is imprinted in the fiber when it is drawn. Backscatter light presents a high repeatability in absent of external effects.**

But there are still more measuring possibilities using this technique. Rayleigh backscatter in optical fiber is caused by random fluctuations in the refractive index profile along the length of the tested fiber. These perturbations, originated during the manufacturing process of the fiber, will behave as very weak and random wavelength FBGs engraved in the fiber all along its length. Shifts in the fiber index of refraction *n* or in the average perturbation period caused by an external stimulus (like strain or temperature) promoted shifts in the local spectral frequency of the Rayleigh backscatter (fig 4). Accumulated changes in the refractive index along the optical path also manifest as a time shift of the Rayleigh backscatter return loss amplitude

pattern. Performing a cross correlation on the backscatter amplitude time domain or frequency domain data accurately measures these spectral and temporal shifts, which are scaled to form distributed temperature or strain measurements.

Consequently, a plain optical fiber behaves as a continuous strain/temperature sensor, with a high spatial accuracy, because it was obtained by interferometric procedures, and with the accuracy in the strain/temperature measurements similar to FBGs. The low power of the reflected signals implies a poor SNR (signal to noise ratio), which can be partially improved by averaging, or repeating the measurements several times, limiting the applications of the technology to almost static tests.

## 3.0 COMPARISON OF TECHNOLOGIES

This comparison must be consider very rough, firstly because these technologies are quite new, less than ten years old, and the equipment's performances and prices are evolving very quickly. Secondly, because the definition of performance specifications for distributed sensors is more difficult than for traditional point sensors, since the performance depends on a combination of related measurement parameters. For example, accuracy depends on the requested spatial resolution, acquisition time, distance range or cumulated loss prior to measurement location.

**Table 1: Comparison of strain distributed sensing technologies.**

| | FBG | BOTDR | BOTDA | OBR |
|---|---|---|---|---|
| **Strain Accuracy** | ± 1 microstrain | ± 30 microstrain | ± 10 microstrain | ± 1 microstrain |
| **Spatial resolution** | Related to grating length | 0,1 m | 0,1 m | 0,001 m |
| **Length range** | Point sensor | 100 Km | 100 Km | 2Km |
| **Acquisition time** | 3 KHz typical Sampling rate | 0-20 minutes | As low as 5 min | Related to accuracy and length. (10 sec typical) |
| **Temperature Accuracy** | ± 0,1 °C | N.A. | ±1-2 °C | ± 0,1 °C |
| **Sellers** | MicronOptics, Fibersensing, Insensys, ,… | Yokogawa,NTT, Sensornet | OZ Optics, Omnisens, Neubrex | LUNA |
| **System costs** | 3.000-15.000 € | Over 100.000€ | Over 200.000 € | Over 100.000 € |

## 4.0 APPLICATIONS OF DISTRIBUTED SENSING

### 4.1 Instrumentation of Structural Tests

The distributed sensing technique may significantly improve the instrumentation of structural tests; instead of bonding a large number of sensors, it will be substituted by bonding one (or several) plain optical fibers in the regions of interest. The main advantage of this technology is that it provides a full coverage of the instrumented area. This issue is of special interest in composite structures, commonly designed with changes of thickness and different stacking sequences. As a consequence, the strain field is not uniform and it is cumbersome to monitor all the critical areas with point strain gauges, since this information is directly obtained with distributed sensing. This technology is also very suitable for detecting local buckling, a problem which presents a great level of difficulty when predicting its character.

In comparison with traditional extensometer sensors, as strain gauges, distributed optical sensors provide a lower price/performance ratio, as it is easy to install, either bonded or embedded, with significant savings in time and money. As no sensor needs to be engraved, standard optical fiber can be used, and it can be obtained with a very competitive price in the market.

In spite of these enormous advantages, this technology has not replaced traditional extensometry, mainly due to two reasons; in first place, the purely static acquisition rate, which limits the technique to static tests. It is possible to increase the acquisition rate by using a special optical fiber much more expensive, but it is still unable to be used for aeronautical testing. The second reason is the directional nature of the optical fiber, which makes it extremely difficult to measure the strain field in more than one direction, whilst it is easy to make a rosette with strain gauges. Currently, the state of art of this technology allows it to be used in structural tests, but always as a support for traditional extensometry.

This technique is already used for structural tests of wind turbine blades. Wind turbine blades are the perfect candidates due to their enormous size, because a high number of sensors required to cover the full structure and the material, with continuous changes of thickness and non uniform properties.

The results of the structural test of a 43 meters long wind turbine blade are presented. Up to six standard optical fibers where bonded at the external surface of a wind turbine blade at the following locations: one in the leading edge, two in the pressure side, one in the suction side, and two each side of the trailing edge (see figure 5). Only one interrogation system was used, the signal was shifted from one fiber to the next one by and optical switch. All these fibers were oriented in the direction of the spar, and run from the root to the edge. Temperature corrections were not needed because the temperature was kept uniform over the structure and constant since the start of load application. In case the temperature would have changed during the tests, a compensation procedure should be done on the data, as with any other strain gages.

The concordance amongst the point data obtained with strain gages and the continuous line obtained with the OBR is excellent; the crooked line is not due to noise, but to the abrupt changes due to ply drops and changes in thickness in the skin of the blade. OBR measurements help the designers detect all the stress concentration areas, even if they were not initially considered of interest. Also, the initiation of the elastic buckling can be clearly detected and located.

Another interesting application under study for wind turbine blades, not related with structural test, is to monitor temperature during the curing along the full structure. One optical fiber can substitute several thermocouples with a better integration. The first results obtained in the laboratory are very promising.

**Figure 5: Structural test of a full wind turbine blade.**

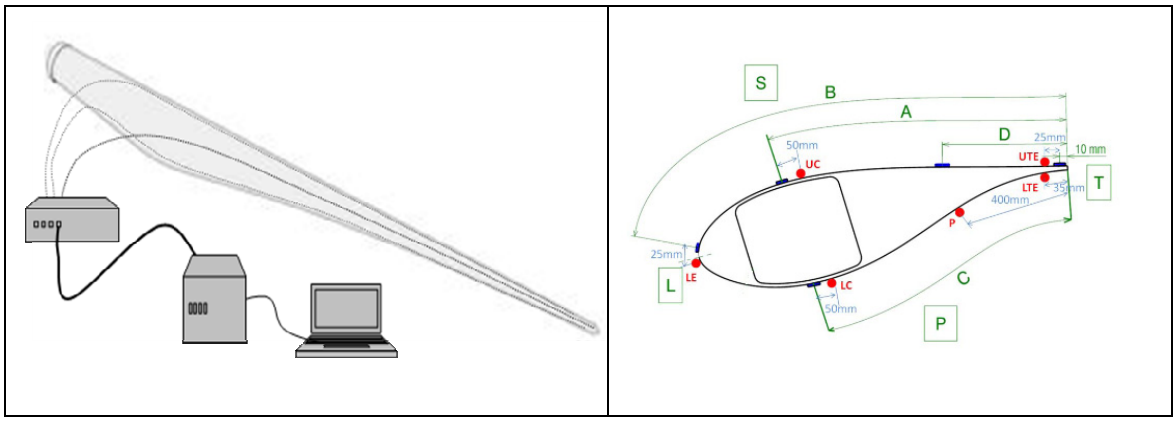


**Figure 6: Scheme of fibers mounted in the full blade (left) and in one transversal section (right).**

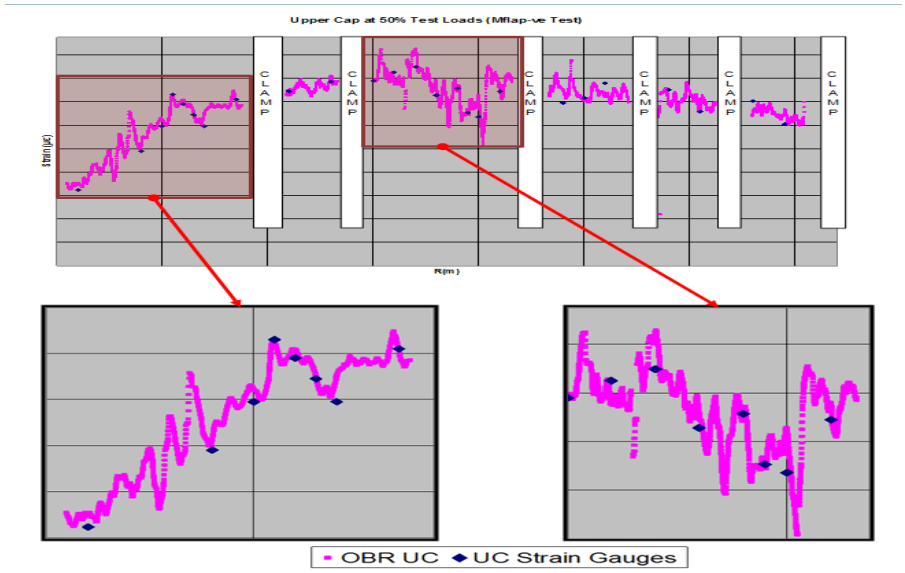


**Figure 7: Strain measurements along the length of the blade).**

## 4.2 Damage detection in Civil Structures

Another field in which distributed sensing can deliver important benefits is civil engineering, since it can be used for monitoring civil structures, such as big buildings, bridges or pipelines. These structures need to be monitored in order to prove their structural safety, and to prevent them from deterioration or damage. One of the key points when monitoring this kind of structures is their large size, bigger than the usual instrumented structures. Unless damages produce a significant change in the stresses path, local sensors, as strain gauges, can only detect damages in their nearest area, and a large amount of sensors is required to cover the full structure.

Distributed optical sensors provide a high density sensor network to cover the full structure at a low price, as standard single-mode fiber is used as sensor. However, the capability to easily manage a huge number of sensors using distributed sensing is not new. Up to now distributed sensing techniques have not found a widespread usage in civil structural applications due to their insufficient resolution and their limitation to be used in static examples to measure average strain, due to the poor resolution of previous distributed techniques.

One of the applications that have attracted most interest is pipeline crack monitoring. Small cracks can be detected due to the large increase of the average strain at the region of the fiber where the crack was produced. Several papers have used this approach; the OBR improves the spatial resolution of the mentioned technologies.

A similar experimental test was carried out on a reinforced concrete slab in the Structural Technology Laboratory of UPC. One fiber was bonded on the surface of a reinforced concrete slab of 5.60x1.60 m. The fiber was bonded along the longitudinal direction, with two lines in the upper side and another two lines bonded on the lower side (Figure 8).

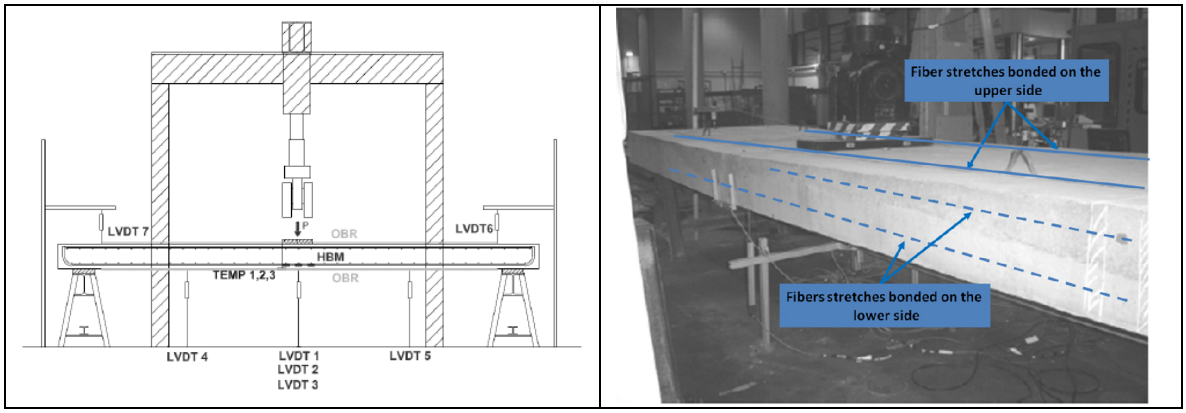


**Figure 8: Test scheme (left). Location of optical fiber on concrete slab right).**

Strain sensors are not commonly used in the surface of concrete slabs since material heterogeneity due to the presence of aggregates of several sizes promotes a non uniform strain field in the surface. In figure 9 the strain field in the upper side at different load levels can be observed. Strain grows uniformly, with irregularities near the load application region.

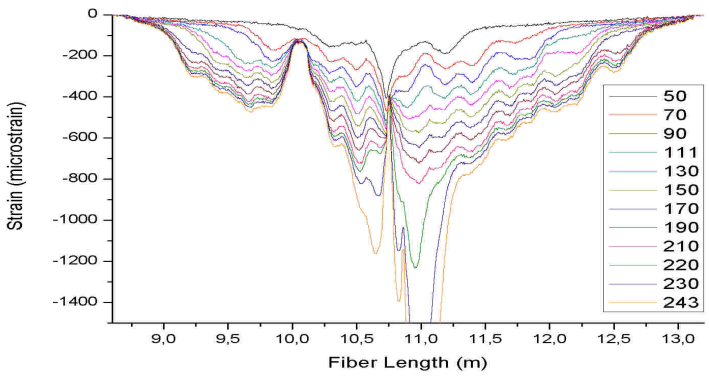


**Figure 9: Strain field in the upper side of the slab at different load levels.**

At the bottom side, tensile stressess promote crack appearance, and the strain chart is quite different. Data measured with optical fibers detects strain concentration due to cracks, even at low load levels. It is possible to track crack appearance with increasing load levels, and detect crack location even in severe cracking conditions (Figure 10 and 11).

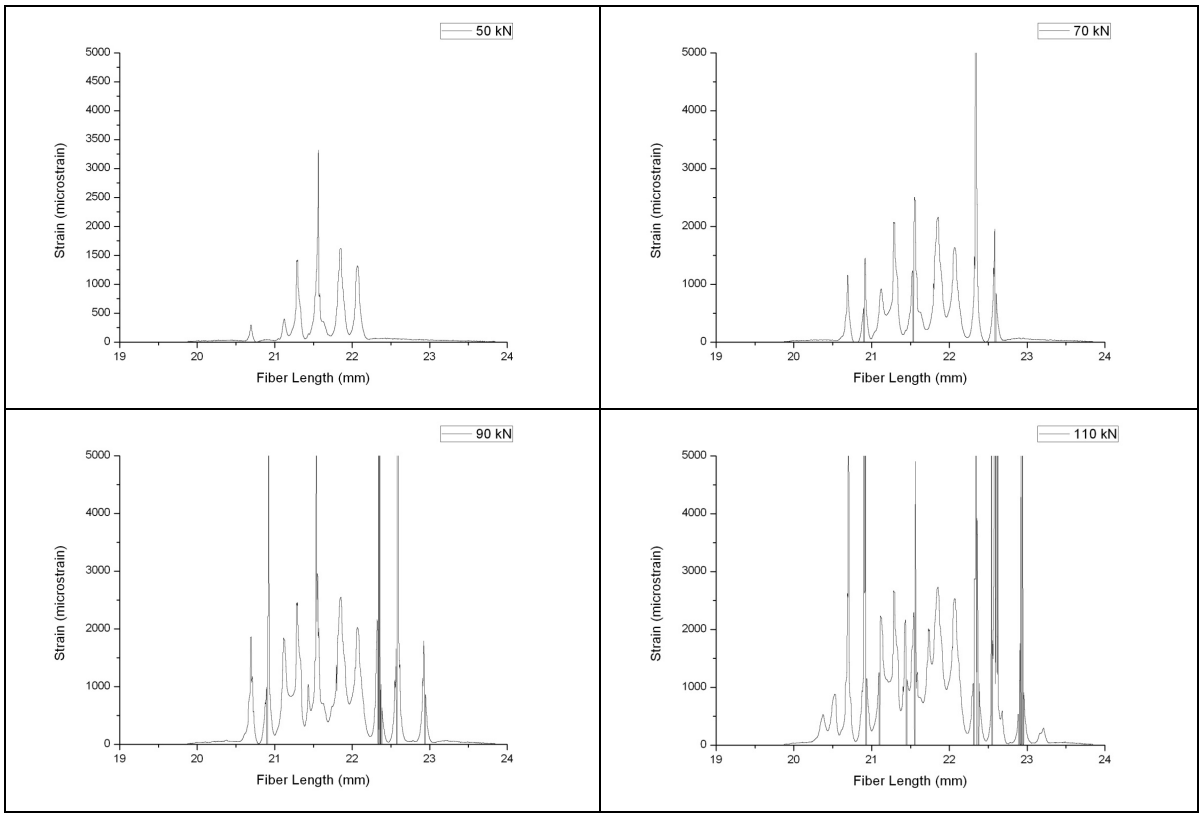


**Figure 10: Strain measured with OBR along the lower side for different load levels: 50kN (up, left), 70kN (up, right), 90kN (down, left) and 110kN (down, right).**

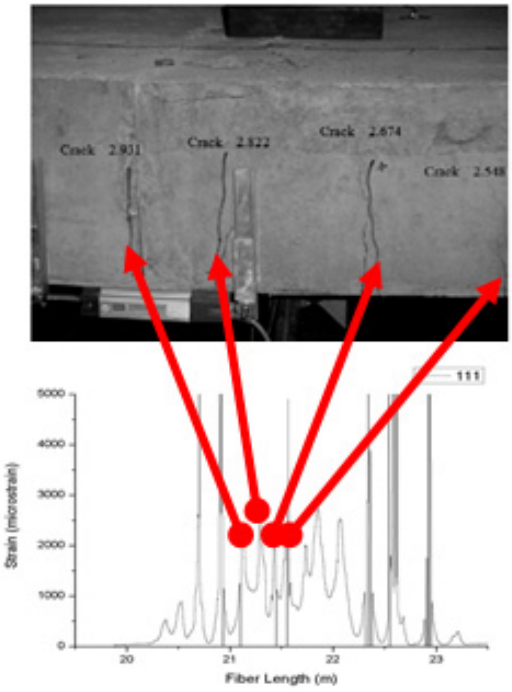


**Figure 11: Correspondence between strain concentration peaks (down) and cracks in the concrete slab.**

## 4.3 Damage Detection in Composites Laminates

Another promising field for this technology is aeronautics. High accuracy in strain resolution and a spatial resolution better than 1 mm allows an ultra high density sensor network with a single optical fiber, with such good performances that it may even detect the strain changes induced by a delamination.

Strain changes induced by a delamination are related to the residual strains built in the laminate during the curing and have only a local influence, limited to the delamination area. For these reasons a high-density strain sensor network is required, and formerly SHM techniques for delamination detection were not based on strain measurements.

To study the changes in the strain field promoted by impact damages, plates 150 mm long and 100 mm wide were manufactured with an embedded optical fiber. Plates were built with carbon/epoxy tape AS4/8552 with $[0_2,90_2,0_2]$ cross ply lay-up. Optical fibers were embedded along the longitudinal central line between plies with the same orientation. The embedded optical fiber has polyimide coating with a final diameter of 140±2 με. This type of coating is recommended for measuring the strain gradients due to their small thickness, as thicker coating can smooth the real strain gradients.

The first plate was subject to a 2.4 J impact at the middle of the plate. With this energy level, fiber C-1 (embedded in the opposite side to the impact) was broken. The strain readings at the other two fibers show a peak in damage location with similar strain level. In Figure 12 the C-Scan inspection after the damage can be observed. The strain field is mainly affected in the delamination area, with a maximum of nearly 500 με. One of the fibers, the one embedded in the middle of the plate, between the 90º plies, presents a strain field variation limited to the delamination area. The other fiber, embedded between two 0º plies, is mainly affected in the delamination area, but strain field changes affect also the close delamination region. With an impact of 4.4 J, all the fibers were broken. Test performed with fibers with acrylate coating of 250 με did not show an improvement of resistance to impacts.

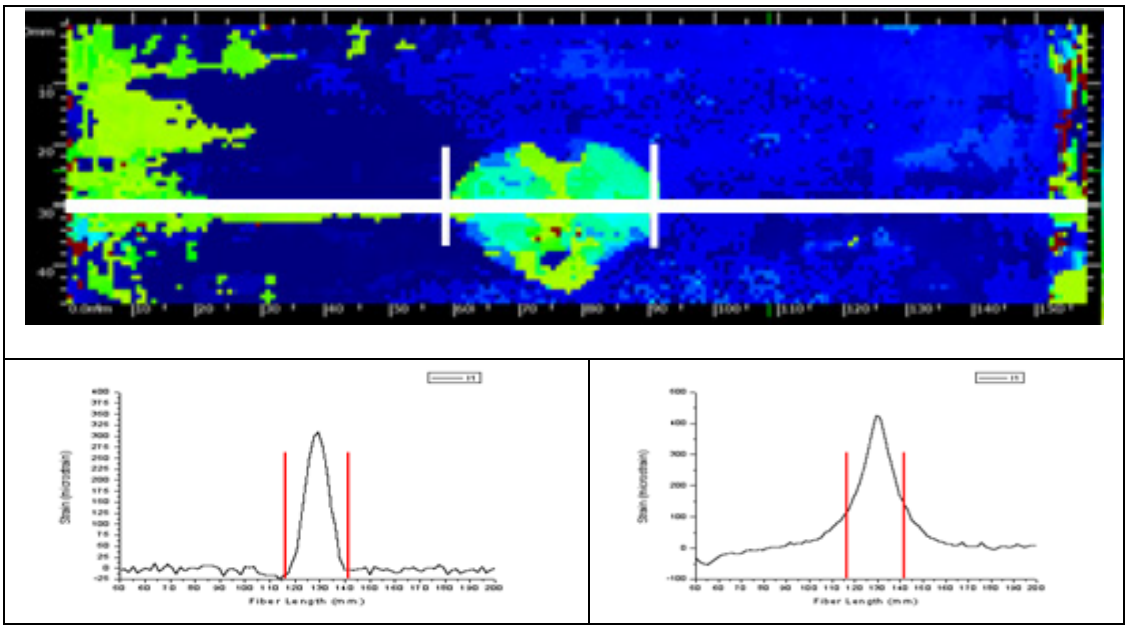

**Figure 12: Ultrasonic inspection C-Scan after 2.4 J impact (up). Strain measures of fibers C-2 (down, left) and C-3 (down, right).**

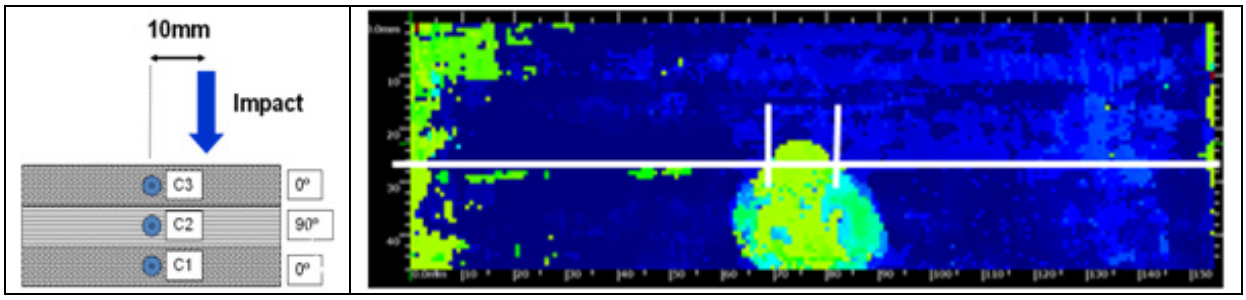


**Figure 13: Scheme of test (left). Ultrasonic inspection C-Scan after 4.4 J impact (right).**

To avoid fiber breakage, impacts were performed 10 mm away from the fiber line (see Figure 13-Left). In this case, a growing delamination was monitored. In spite of the delamination size growing, the fiber length inside the delamination remained nearly constant. Figure 14 shows the strain along the different fibers: strain fields are similar in all of them, and present a maximum strain level in the delamination area. In these tests, all of the fibers show also an influence in the close strain field. Additionally, impact energy has no effect in the strain field level. Impacts were done for increasing energy levels (2.4, 4.4, 6.3 and 12 J).

Strain results can be explained by the influence of the cracks induced in the 90º plies, as the residual strain of these plies in the direction of the fiber is mainly compression. After the cracks appear, residual stresses are relaxed and affect the 0º plies too.

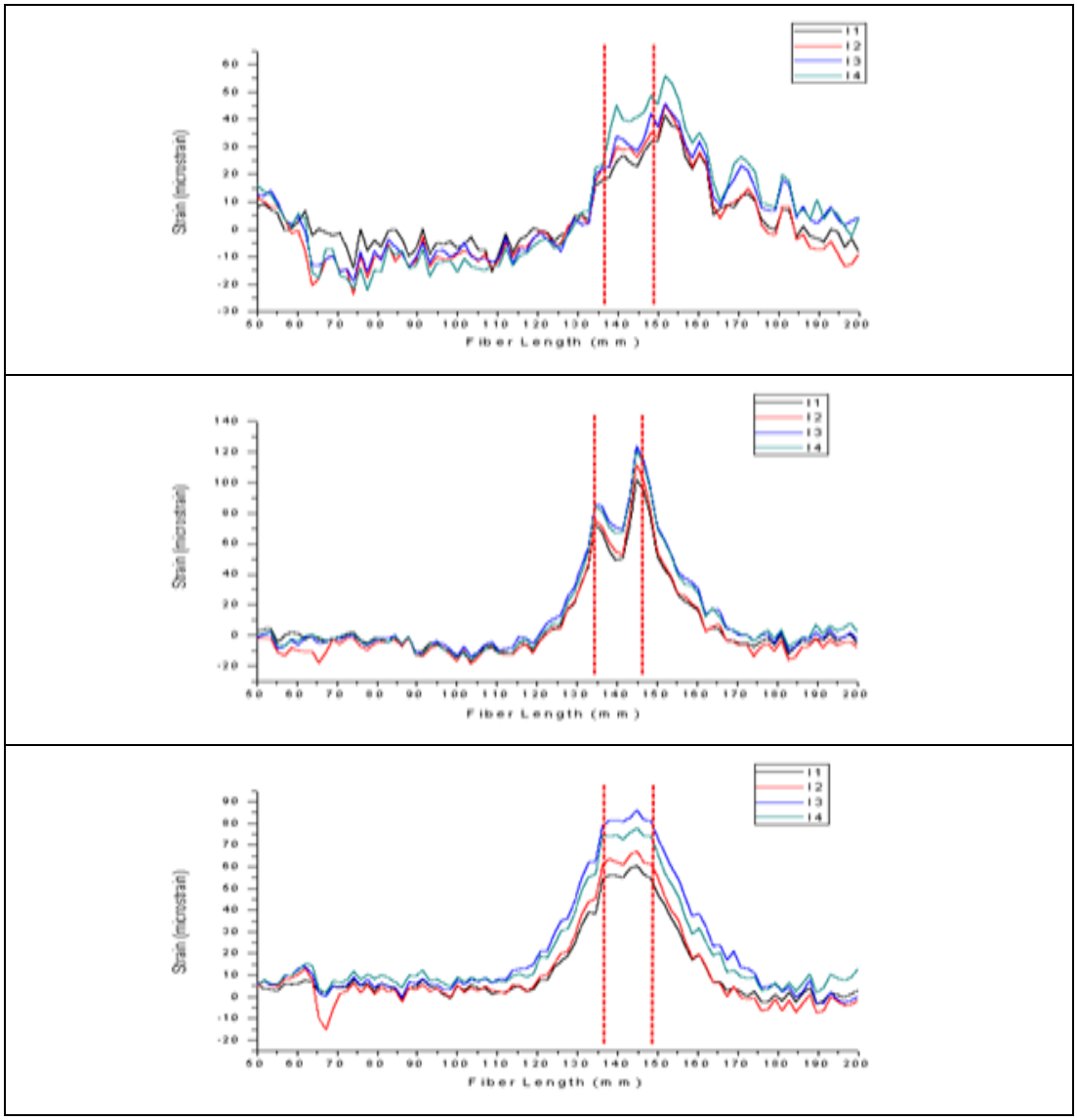


**Figure 14: Strain distribution along the fiber after different impact levels for fiber C-1 (up), C-2 (middle) and C3 (down).**

Strain measurements obtained from the full surface can be used to create a strain map of the structure. In case that a damage promotes a change in the strain field, it is possible to obtain an image that represents the state of the structure. Figure 16 shows the effect of a delamination in a cross ply laminate of 200x200 mm. Strain data was obtained from a fiber in a zig-zag configuration that covered one of the sides.

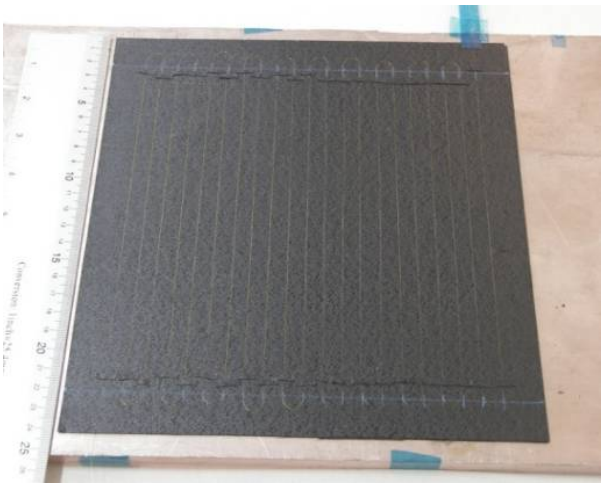

**Figure 15: Fiber in a uniform zig-zag distribution in a composite laminate.**

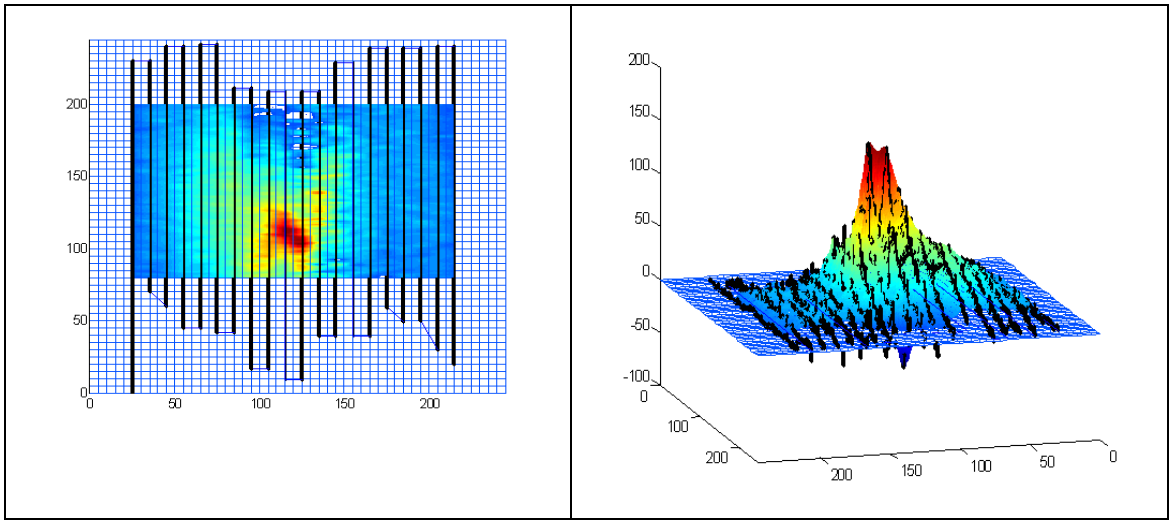


**Figure 16: Strain map due to a delamination in 2D (left). And 3D (right).**

It has to be emphasized that only when the damage produces a change in the local strains in a region crossed by a fiber, it may be detected by this approach. It is demonstrated by the next experiment.

An optical fiber is bonded at the surface of a composite laminate. Firstly, to identify the position, it is enough to get a reading with two fingers on the fiber, the local increase of temperature are clearly defined (figure 17a). Then, an impact of 40 Joules is done 40 mm away from the fiber; a second reading is obtained (figure 17b). The strains along the fiber have not changed, only a noise of 2 microstrains is detected. Next, an impact of 30 Joules, 10 mm away from the fiber is done, and a permanent change in the strains at the optical fiber is registered (figure 17c). Another impact is done, again 10 mm from the fiber and a few cms away from the former impact. Again a permanent strain is seen in the fiber, together with the peak from the former impact.

Looking at the physical damage done in the laminate (figure 18), the 40 Joules impact was strong enough to penetrate the laminate, but it did not caused a change in the strains 40 mm away. The other two impacts of 30 Joules only produced visible denta at the laminate, and a permanent change in the residual strains in a zone 20 mm around the impacts.

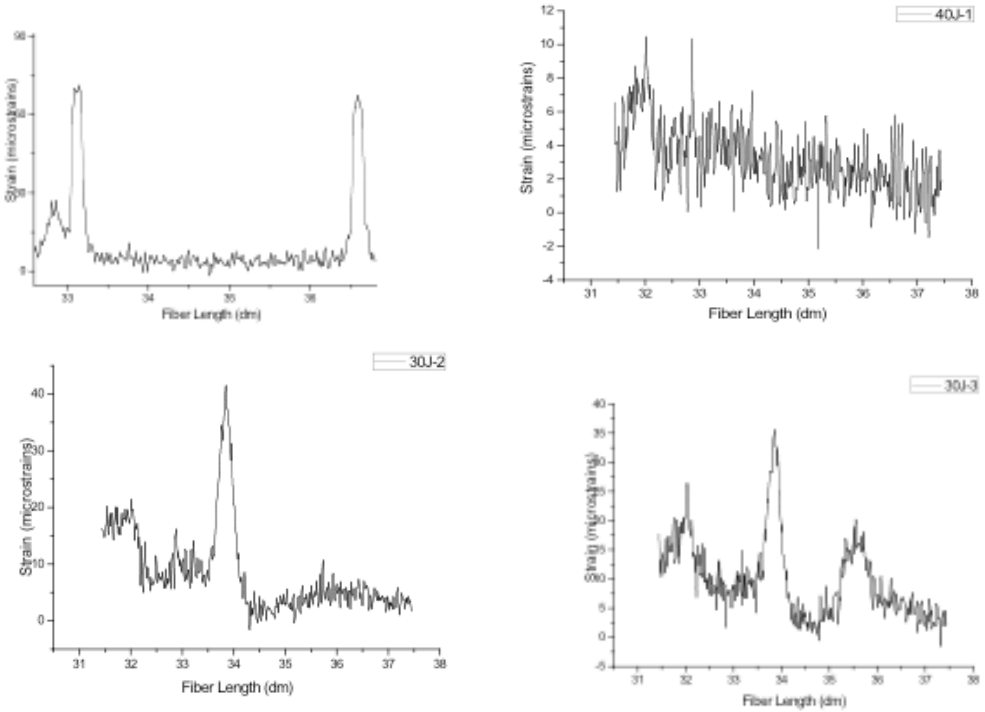


**Figure 17: Strains along the optical fiber. Upper left: Local temperature increases, for localization. Upper right: Residual strains after a 40 J impact, 40 mm away from the fiber. Lower left: residual strains after a impact 30 J, 10 mm away from the fiber. Lower right: Strains after a second impact of 30 J, at another position.**

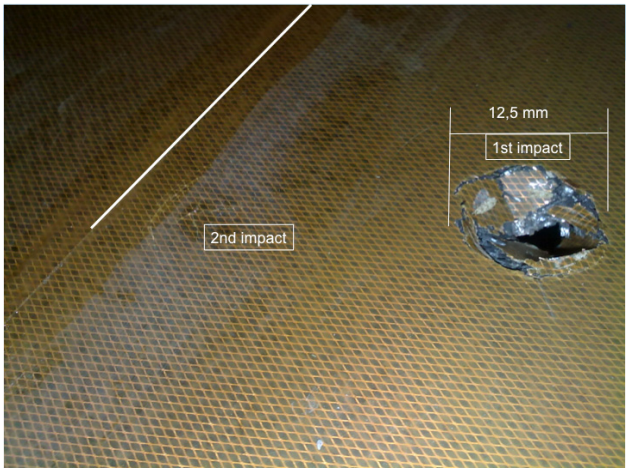


**Figure 18: Image of the positions and damages done by the impacts on the laminate.**

## 4.4 Monitoring the Stringer Debonding in Composites Structures

Most of the aeronautical structures are built as stiffened panels and shells, usually by a cobonding process for composite materials (skin is uncured, stiffener are added as cured rigid elementals). This is an efficient way to achieve a very high level of structural integration, but still an issue is unsolved: the stiffener run-away, or debonding starting at the tip. Classical way to solve it is by increasing the foot size (which makes more expensive the manufacturing of the stiffener), and by 'chicken rivets'. Nevertheless, it needs to be inspected in service, so an automated procedure to check the structural integrity is highly desirable.

At the European project SARISTU (Smart Aircraft Structures) an activity is carried out to solve this issue, with different approaches: A) Distortion of the spectral shape of embedded FBGs. B) Fiber optic distributed sensing.

This second approach has shown to be quite resolute to detect the initiation and advancement of stringer debonding.

### Experimental Setup

A flat laminate with an embedded optical fiber, similar to the one presented at figure 15, was prepared, the stiffener was added and the whole set was cured (fig 19, left). To promote a progressive debonding, a mechanical artifact was attached (fig 19 right). With the screw, the crack was grown, then unloaded again.

The occurrence of the crack has locally changed the strain state at the flat laminate, as measured by the embedded fiber and plotted at figure 20, left. The debonding has created an area of compressive strains just below the stringer, the maximum value not very high ( -80 MPa), but clearly detectable. The crack front is clearly defined, and it is coincident with the findings obtained by ultrasonic inspection (figure 20, right). Similar results are obtained at every step of the crack growth, which demonstrates the reliability of the technique.

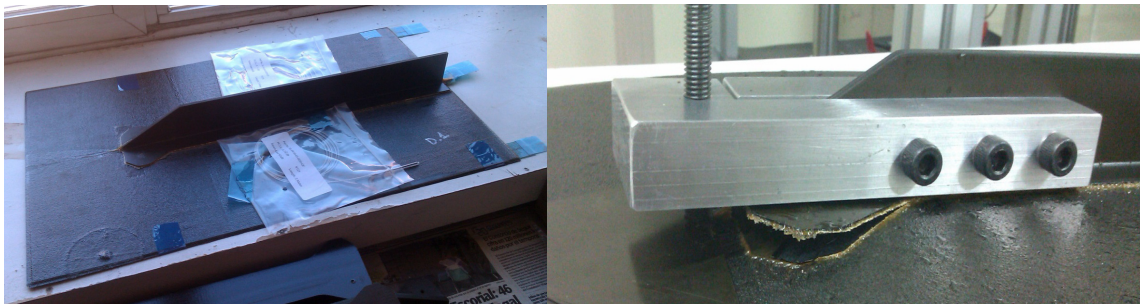

**Figure 19: Manufacturing a cobonded stiffened panel with an embedded optical fiber, and artifact to promote a progressive debonding.**

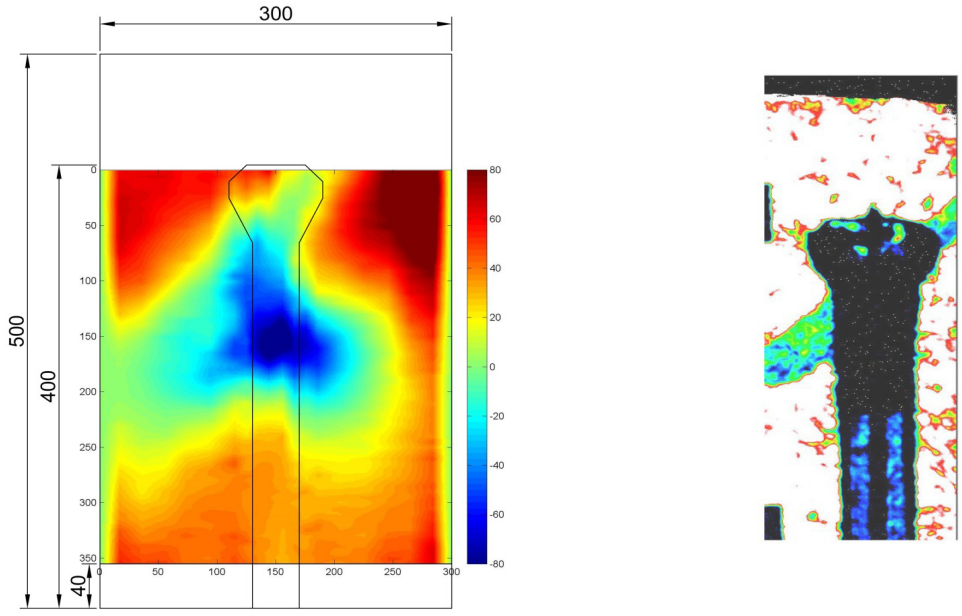


**Figure 20: Map of the strains (left) and C-Scan image of the ultrasonic inspection (right).**

## 5.0 CONCLUSIONS

While FBG provide local strain measurements, similarly to strain gages, new possibilities are opened by the distributed sensing, giving the information all along the optical fiber. Structural tests may be instrumented with greater details, and crack occurrence will be easily detected, as long as the crack crosses the optical fiber path.

The changes in the strain field are very intense at the tip of the cracks, but smooth out very quickly, a few cms away the changes are negligible, so it is very difficult to get information on damage occurrence just from strain measurements; Fiber optic sensors are just strain sensors, so its usage for damage detection is very limited, still under development. Currently, three main approaches for detecting damage from strain measurements are being investigated:

1) High resolution fiber optic distributed sensing ( OFDR Rayleigh scattering). When the crack crosses the optical fiber, a high strain spot is detected. This technique is applicable to cover high risk areas, like stiffeners debonding.
2) Strain mapping with a dense sensor network , either distributed OF or highly multiplexed FBGS. Multivariate statistical analysis tools, like PCA, it is needed to extract the meaningful deviations, and to distinguish damages from loads or environmental factors changes.
3) Hybrid FBG/PZT systems. FBGs must detect the ultrasonic elastic waves, high sensitive and high speed interrogation systems are required.

## 6.0 BIBLIOGRAPHY

1. B. A. Childers, M. E. Froggatt, S. G. Allison, T.C. Moore, D.A. Hare, C.F. Batten, D.C. Jegley, "Use of 3000 Bragg grating strain sensors distributed on four eight-meter optical fibers during static load testing of a composite structure," Proceedings, SPIE's 8th Annual International Symposium on Smart Structures and Materials in Newport Beach, California, Vol. 4332, Paper No. 4332-17, March 2001.

2. Güemes, JA, Fernandez-Lopez, A, Soller B "Optical Fiber Distributed Sensing. Physical Principles and Applications" J. *Structural Health Monitoring*, Vol. 9, No. 3, 233-245 (2010).